

Supporting Information for:

Conformational Diversity and Enantioconvergence in
Potato Epoxide Hydrolase 1

P. Bauer¹, Å. Janfalk Carlsson², B. A. Amrein¹, D. Dobritzsch^{2,*}, M. Widersten^{2,*} and
S. C. L. Kamerlin^{1,*}

1. Science for Life Laboratory, Department of Cell and Molecular Biology, Uppsala University, BMC Box 596, S-751 24 Uppsala, Sweden. 2. Department of Chemistry-BMC, Uppsala University, BMC Box 576, S-751 23 Uppsala, Sweden

Corresponding Author Email Addresses:

doreen.dobritzsch@kemi.uu.se; mikael.widersten@kemi.uu.se; kamerlin@icm.uu.se

Table of Contents

S1. Calibrating the Relevant Reference Reactions for the EVB Simulations	S4
S2. References	S5
S3. Figures & Tables	S8
Figure S1: RMSD plots of the protein backbone during equilibration runs for wild-type StEH1 in complex with (R)- and (S)-SO.	S8
Figure S2: RMSD plots of the protein backbone during equilibration runs for the R-C1B1 StEH1 variant in complex with (R)- and (S)-SO.	S9
Figure S3: Observed transient rates, k_{obs} , in the approach to the steady state, and amplitudes of Trp fluorescence quenching during the steady state phase.	S10
Figure S4: RMSD plots of the substrate during equilibration runs for wild-type StEH1 in complex with (R)- and (S)-SO.	S11
Figure S5: RMSD plots of the substrate during equilibration runs for the R-C1B1 StEH1 variant in complex with (R)- and (S)-SO.	S12
Figure S6: Key enzyme-substrate distances during equilibration runs for wild-type StEH1 in complex with (R)- and (S)-SO.	S13
Figure S7: Key enzyme-substrate distances during equilibration runs for the R-C1B1 StEH1 variant in complex with (R)- and (S)-SO.	S14
Figure S8: Representative transition state structures for the formation of the alkyl enzyme intermediate during the StEH1-catalyzed hydrolysis of (R)- and (S)-SO.	S15
Figure S9: Representative structures of the alkyl enzyme intermediate formed during the StEH1-catalyzed hydrolysis of (R)- and (S)-SO.	S16
Figure S10: Representative transition state structures for the formation of the alkyl enzyme intermediate during the R-C1B1-catalyzed hydrolysis of (R)- and (S)-SO.	S17
Figure S11: Representative structures of the alkyl enzyme intermediate formed during the R-C1B1-catalyzed hydrolysis of (R)- and (S)-SO.	S18
Table S1: Comparison of the EVB and experimental or DFT energetics of the uncatalyzed hydrolyses of (R)- and (S)-SO in aqueous solution.	S19
Table S2: Average values of substrate RMSD and key enzyme-substrate distances during our equilibration runs for all systems.	S20

Table S3: Absolute energies, entropies and frequencies for DFT calculations of the uncatalyzed hydrolyses of (<i>R</i>)- and (<i>S</i>)-SO in aqueous solution.	S21
S4. Empirical Valence Bond Parameters Used in This Work	S22
Table S4: EVB parameters used in this work.	S22
Figure S12: Structures of the different VB states used in this work.	S23
Table S5: Van der Waals parameters used for atoms constituting the reacting system.	S24
Table S6: Atom types in different VB states.	S25
Table S7: Atomic charges of the reacting system.	S26
Table S8: Bond parameters for the covalent bonds of the reacting system.	S27
Table S9: Bond types in different VB states.	S28
Table S10: Angle parameters for bending adjacent bonds in the reacting system.	S30
Table S11: Angle types of the different VB states.	S31
Table S12: Torsion parameters used in the reacting system.	S33
Table S13: Torsion types in the different VB states.	S34
Table S14: Improper torsion parameters used in the reacting system.	S37
Table S15: Improper torsions parameters of the different VB states	S37
S5. Cartesian Coordinates for Key Stationary Points	S38

S1. Calibrating the Relevant Reference Reactions for EVB Simulations

As shown in **Figure 5** of the main text, two independent reacting steps need to be taken into account when calibrating the uncatalyzed hydrolysis of styrene oxide (SO), specifically the initial ring opening step and the subsequent hydrolysis of the resulting intermediate. As discussed in detail in the Supporting Information of our previous work¹, despite extensive experimental data on acid- and base-catalysed epoxide hydrolysis²⁻¹⁰, there exist no data for our model system which involves the attack of acetate nucleophile on SO to form an oxirane intermediate. This species will be highly unfavourable in aqueous solution, and therefore this pathway is unlikely to be experimentally observed; however, experimental data suggests that StEH1 is able to exploit a strategically located oxyanion hole to stabilize this species in its active site as an intermediate along the pathway for the enzyme-catalysed reaction¹¹. The essence of the EVB approach is based on using a common “chemically-filtered” reference state when fitting the parameters of the reference reaction in aqueous solution (see discussion in ref. ¹²), *i.e.* using the same reaction mechanism for both the catalysed and uncatalyzed reactions. Due to the lack of experimental data for this process, we fit our empirical valence bond (EVB) parameters instead to higher-level quantum chemical calculations using density functional theory (DFT), following the protocol used in our recent study of the StEH1-catalyzed hydrolysis of trans-stilbene oxide (TSO)¹. In addition, unlike TSO, styrene oxide is no longer symmetrical and therefore each attack at each carbon atom of each enantiomer had to be considered explicitly. As in our previous study¹, we used the B3LYP functional¹³⁻¹⁵ without any empirical dispersion correction, in order to be able to directly compare to previous work¹⁶⁻¹⁸ and also due to the problems involved in treating anionic nucleophiles with implicit solvent models (see discussion in ref. ¹⁹ and references cited therein), in order to not correct for one error and introduce another. While the resulting absolute energetics are not necessarily perfect, our main interest is in the relative energies between attack at different carbon atoms and enantiomers, and this should be reliable (as also observed in our previous study¹).

All transition state geometries were optimized at the B3LYP/6-31+G* level of theory, followed by a single point correction using the larger 6-311+G* basis set in order to correct for the energies and obtain the vibrational frequencies. Solvent was treated implicitly using the C-PCM solvent model as implemented in Gaussian 09 Rev. C01²⁰. Our transition states were

confirmed to be real saddle points that correspond to the correct reaction coordinate through analysis of the vibrational frequencies, as well as following the intrinsic reactant coordinate (IRC)^{21, 22} to minima in either direction and performing a final, unrestrained geometry optimization on the IRC minima in order to ensure the correct stationary points are obtained.

The resulting relative and absolute energetics are shown in **Tables S1** and **S3**, relative to the sum energies of the fragments at infinite separation. For our initial calculations (**Table S1**) we considered both possible SO conformations shown in **Figure 4** of the main text for each enantiomer. However, since these two conformations should be energetically identical in aqueous solution, any calculated difference in energy between them is due to simulation artefacts, and we thus used only the energies of the lowest energy SO-conformation for subsequent calibration of our EVB simulations (**Table S1**). The second reaction step is far easier to calibrate due to the extensive experimental data available for ester hydrolysis reactions²³⁻²⁵. Here, the energetics of the uncatalyzed reaction should be independent of enantiomer and binding mode, and thus we fit the energetics of the hydrolysis step to an activation barrier of 19.0 kcal mol⁻¹ and a reaction free energy of 10.0 kcal mol⁻¹ for all species, as per the derivation provided in the **Supporting Information** of our previous study¹.

Note that the background reaction in aqueous solution **is only presented here in order to have a common reference point for all enzyme-catalysed reactions**. By using a common reference point for multiple enantiomers, ring opening positions and enzyme variants, it is possible to directly compare the energetics of the different possibilities for the enzyme catalysed reaction, even if the precise energetics of the corresponding reaction in aqueous solution can be uncertain due to lack of direct experimental data.

S2. References

1. B. A. Amrein, P. Bauer, F. Duarte, Å. Janfalk Carlsson, A. Naworyta, S. L. Mowbray, M. Widersten and S. C. L. Kamerlin, *ACS Catal.*, 2015, 5, 5702-5713.
2. N. S. N. Isaacs, K., *Can. J. Chem.*, 1968, 46, 1043-1046
3. J. Biggs, N. B. Chapman and V. Wray, *J. Chem. Soc. B* 1971, 66-71.
4. E. Y. Lau, Z. E. Newby and T. C. Bruice, *J. Am. Chem. Soc.*, 2001, 123, 3350-3357.
5. J. Koskikallio and E. Whalley, *Trans. Faraday Soc.*, 1959, 55, 815-823.
6. J. G. Pritchard and F. A. Long, *J. Am. Chem. Soc.*, 1956, 78, 2667-2670.

7. F. A. Long, J. G. Pritchard and F. E. Stafford, *J. Am. Chem. Soc.*, 1957, 79, 2362-2364.
8. F. A. Long and J. G. Pritchard, *J. Am. Chem. Soc.*, 1956, 78, 2663-2667.
9. R. C. D. Muniz, S. A. A. de Sousa, F. D. Pereira and M. M. C. Ferreira, *J. Phys. Chem. A*, 2010, 114, 5187-5194.
10. J. G. Pritchard and F. A. Long, *J. Am. Chem. Soc.*, 1956, 78, 6008-6013.
11. L. T. Elfström and M. Widersten, *Biochemistry*, 2006, 45, 205-212.
12. A. Warshel, P. K. Sharma, M. Kato, Y. Xiang, H. B. Liu and M. H. M. Olsson, *Chem. Rev.*, 2006, 106, 3210-3235.
13. A. D. Becke, *J. Chem. Phys.*, 1993, 98, 5648-5652.
14. C. Lee, W. Yang and R. G. Paar, *Phys. Rev. B*, 1988, 37, 785-789.
15. S. H. Vosko, L. Wilk and M. Nusair, *Can. J. Phys.*, 1980, 58, 1200-1211.
16. K. H. Hopmann and F. Himo, *Chemistry*, 2006, 6, 6898-6909.
17. K. H. Hopmann and F. Himo, *J. Phys. Chem. B*, 2006, 110, 21299-21310.
18. R. Lonsdale, S. Hoyle, D. T. Grey, L. Ridder and A. J. Mulholland, *Biochemistry*, 2012, 51, 1774-1786.
19. F. Duarte, T. Geng, G. Marloie, A. O. Al Hussain, N. H. Williams and S. C. L. Kamerlin, *J. Org. Chem.*, 2014, 79, 2816-2828.
20. M. J. T. Gaussian 09 Rev. C01. Frisch, G. W.; Schlegel, H. B.; Scuseria, G. E.; Robb, M. A.; Cheeseman, J. R.; Scalmani, G.; Barone, V.; Mennucci, B.; Petersson, G. A.; Nakatsuji, H.; Caricato, M.; Li, X.; Hratchian, H. P.; Izmaylov, A. F.; Bloino, J.; Zheng, G.; Sonnenberg, J. L.; Hada, M.; Ehara, M.; Toyota, K.; Fukuda, R.; Hasegawa, J.; Ishida, M.; Nakajima, T.; Honda, Y.; Kitao, O.; Nakai, H.; Vreven, T.; Montgomery, J. A., Jr.; Peralta, J. E.; Ogliaro, F.; Bearpark, M.; Heyd, J. J.; Brothers, E.; Kudin, K. N.; Staroverov, V. N.; Kobayashi, R.; Normand, J.; Raghavachari, K.; Rendell, A.; Burant, J. C.; Iyengar, S. S.; Tomasi, J.; Cossi, M.; Rega, N.; Millam, M. J.; Klene, M.; Knox, J. E.; Cross, J. B.; Bakken, V.; Adamo, C.; Jaramillo, J.; Gomperts, R.; Stratmann, R. E.; Yazyev, O.; Austin, A. J.; Cammi, R.; Pomelli, C.; Ochterski, J. W.; Martin, R. L.; Morokuma, K.; Zakrzewski, V. G.; Voth, G. A.; Salvador, P.; Dannenberg, J. J.; Dapprich, S.; Daniels, A. D.; Farkas, Ö.; Foresman, J. B.; Ortiz, J. V.; Cioslowski, J.; Fox, D. J. Gaussian, Inc., Wallingford CT, 2009.
21. H. P. Hratchian and H. B. Schlegel, *J. Chem. Phys.*, 2004, 120, 9918-9924.

22. H. P. Hratchian and H. B. Schlegel, *J. Chem. Theory and Comput.*, 2005, 1, 61-69.
23. W. P. Jencks and J. Carriuolo, *J. Am. Chem. Soc.*, 1961, 83, 1743–1750.
24. M. L. Bender and H. D. A. Heck, *J. Am. Chem. Soc.*, 1967, 89, 1211–1220.
25. R. A. McClelland, V. M. Kanagasabapathy and S. Steenken, *Can. J. Chem.*, 1990, 68, 375-382.
26. A. Warshel, *Computer Modeling of Chemical Reactions in Enzymes and Solutions*, Wiley, New York, 1991.
27. S. C. L. Kamerlin and A. Warshel, *WIREs Comput Mol Sci*, 2011, 1, 30-45.
28. A. Shurki, E. Derat, A. Barrozo and S. C. L. Kamerlin, *Chem. Soc. Rev.*, 2015, 44, 1037-1052.

S3. Figures & Tables

Figure S1: Plots of the RMSD of all backbone C_α atoms during the equilibration of wild-type StEH1 in complex with **(A,B)** (*R*)- and **(C,D)** (*S*)-SO bound in **Mode1** and **Mode2** respectively (for a definition of the two binding modes see **Figure 4** of the main text). RMSD plots are shown in Å, relative to the original crystal structure.

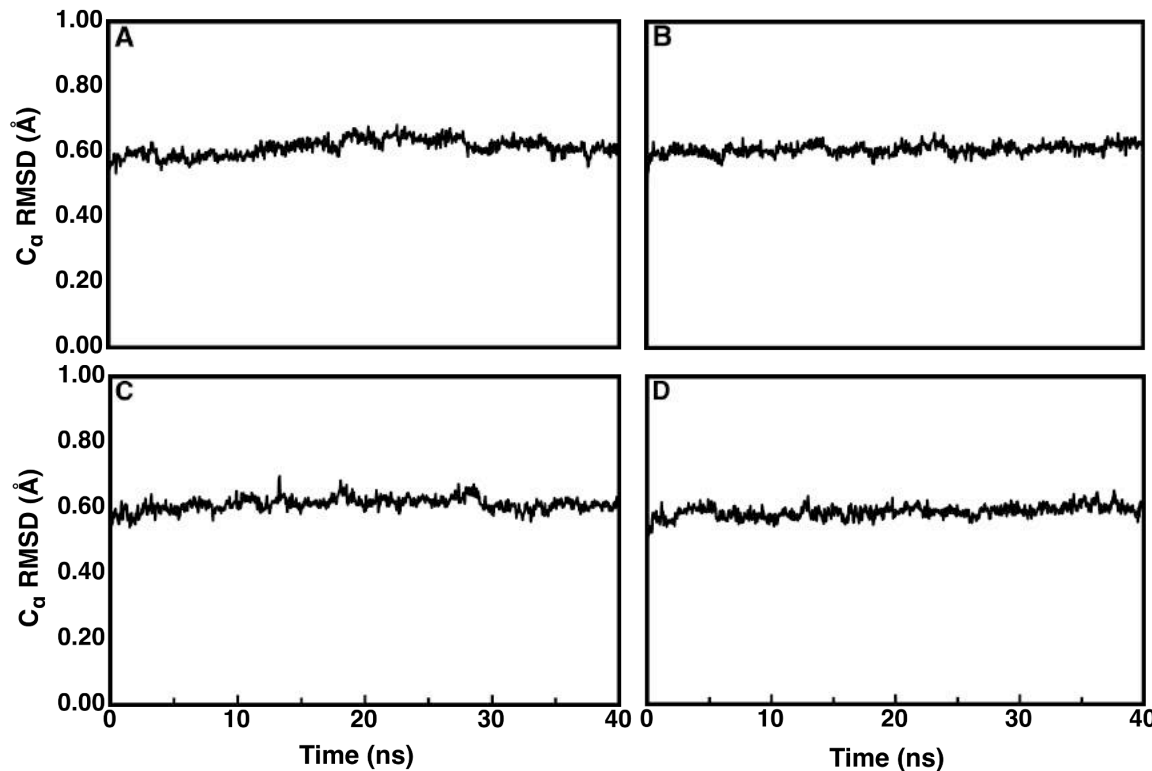


Figure S2: Plots of the RMSD of all backbone C_α atoms during the equilibration of the R-C1B1 variant of StEH1 in complex with **(A,B)** (*R*)- and **(C,D)** (*S*)-SO bound in **Mode1** and **Mode2** respectively (for a definition of the two binding modes see **Figure 4** of the main text). RMSD plots are shown in Å, relative to the original crystal structure.

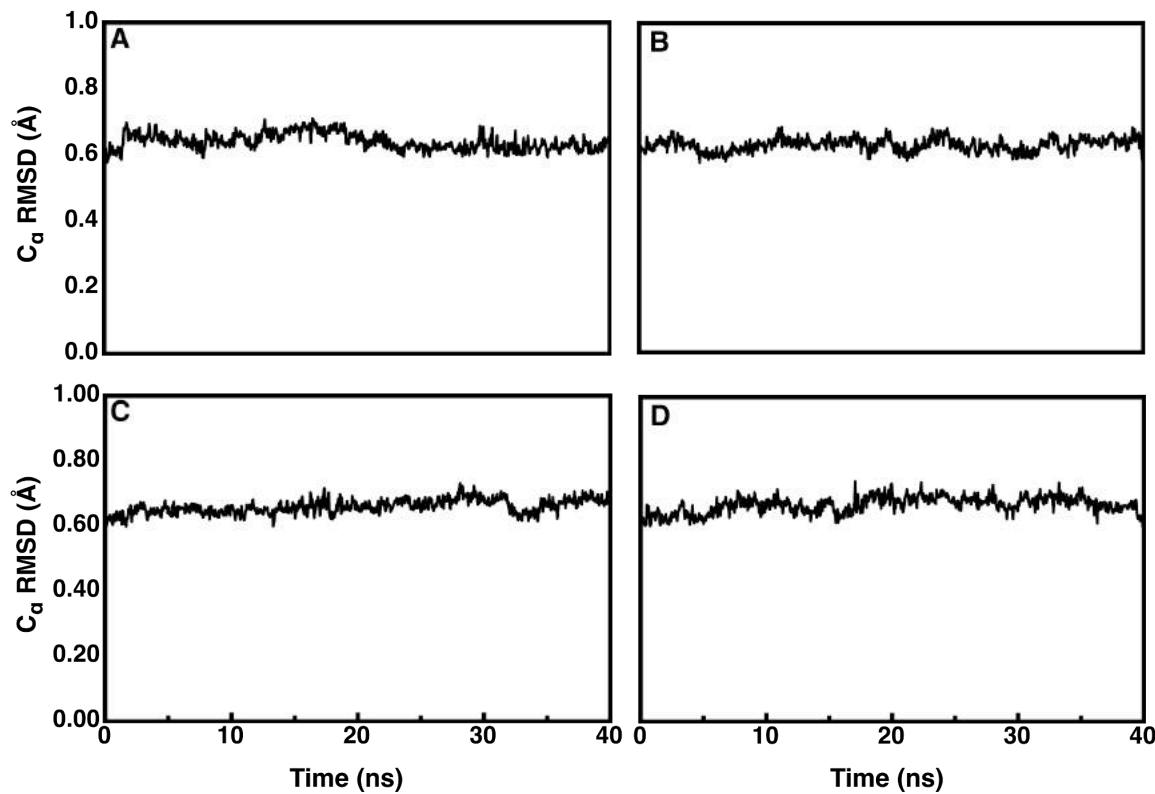


Figure S3: (A) Observed transient rates, k_{obs} , in the approach to the steady state, and (B) amplitudes of Trp fluorescence quenching during the steady state phase. Squares, (*S*)-SO and circles, (*R*)-SO. See the **Methodology** section of the main text for the experimental details.

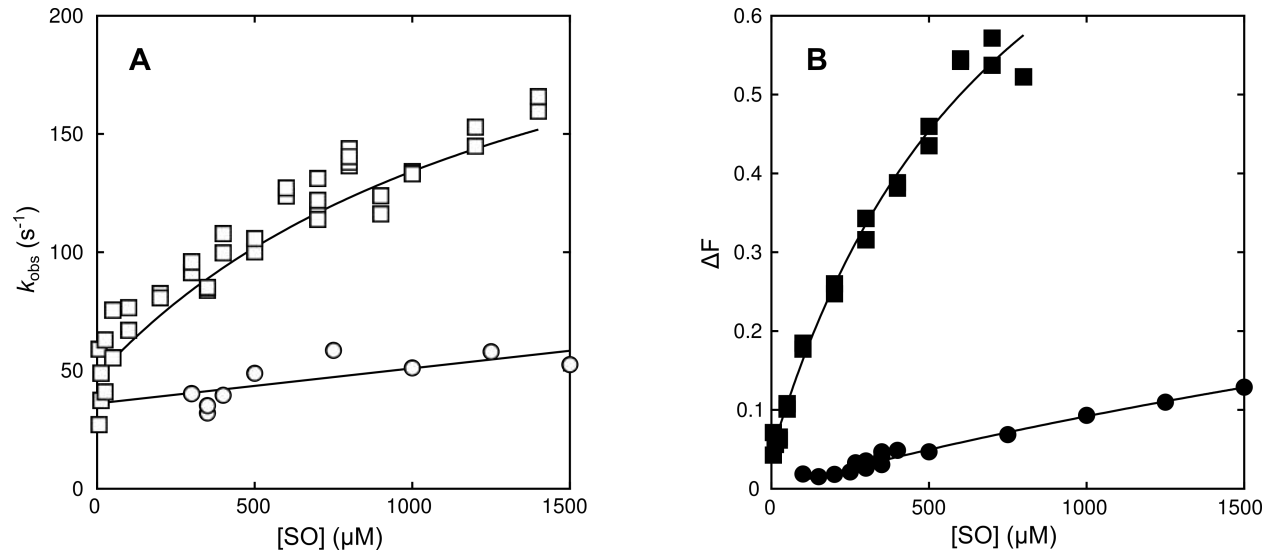


Figure S4: Plots of substrate RMSD during the equilibration of wild-type StEH1 in complex with (A,B) (*R*)- and (C,D) (*S*)-SO bound in **Mode1** and **Mode2** respectively (for a definition of the two binding modes see **Figure 4** of the main text). RMSD plots are shown in Å, relative to the starting structure.

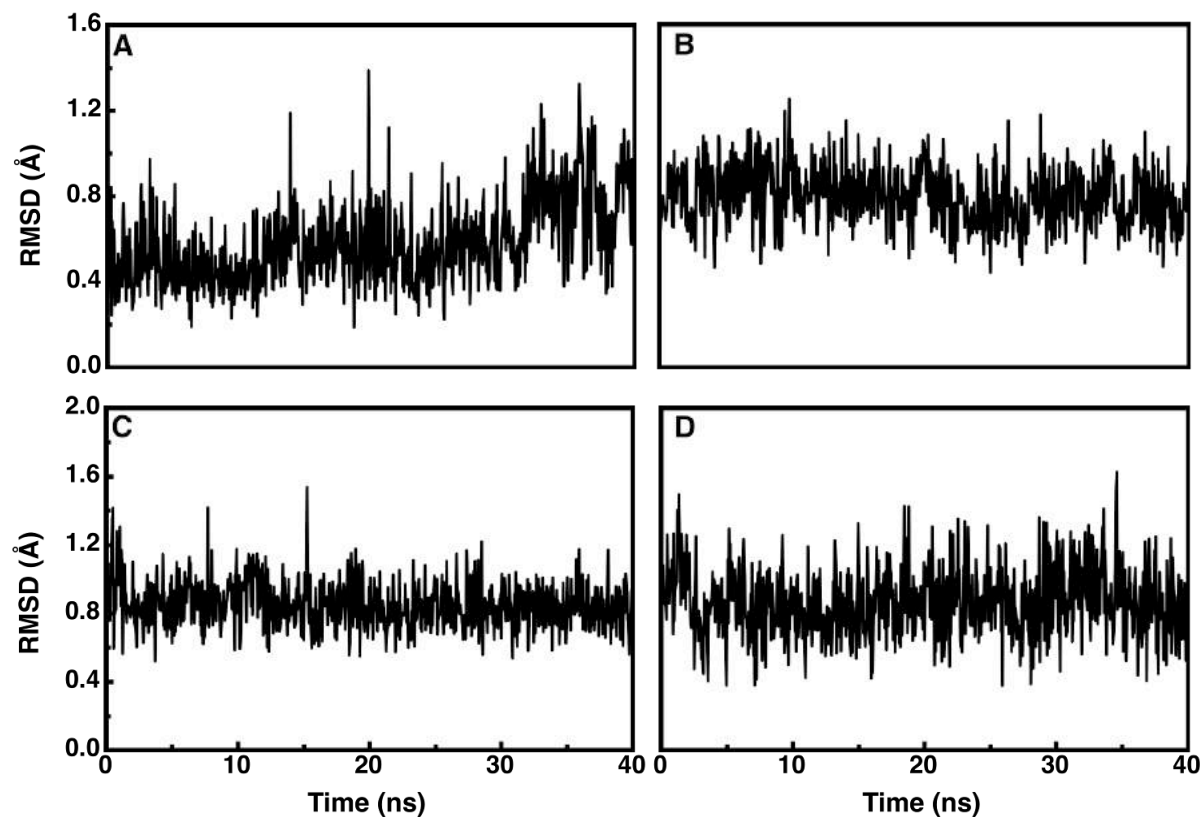


Figure S5: Plots of substrate RMSD during the equilibration of the R-C1B1 variant of StEH1 in complex with **(A,B)** (*R*)- and **(C,D)** (*S*)-SO bound in **Mode1** and **Mode2** respectively (for a definition of the two binding modes see **Figure 4** of the main text). RMSD plots are shown in Å, relative to the original crystal structure.

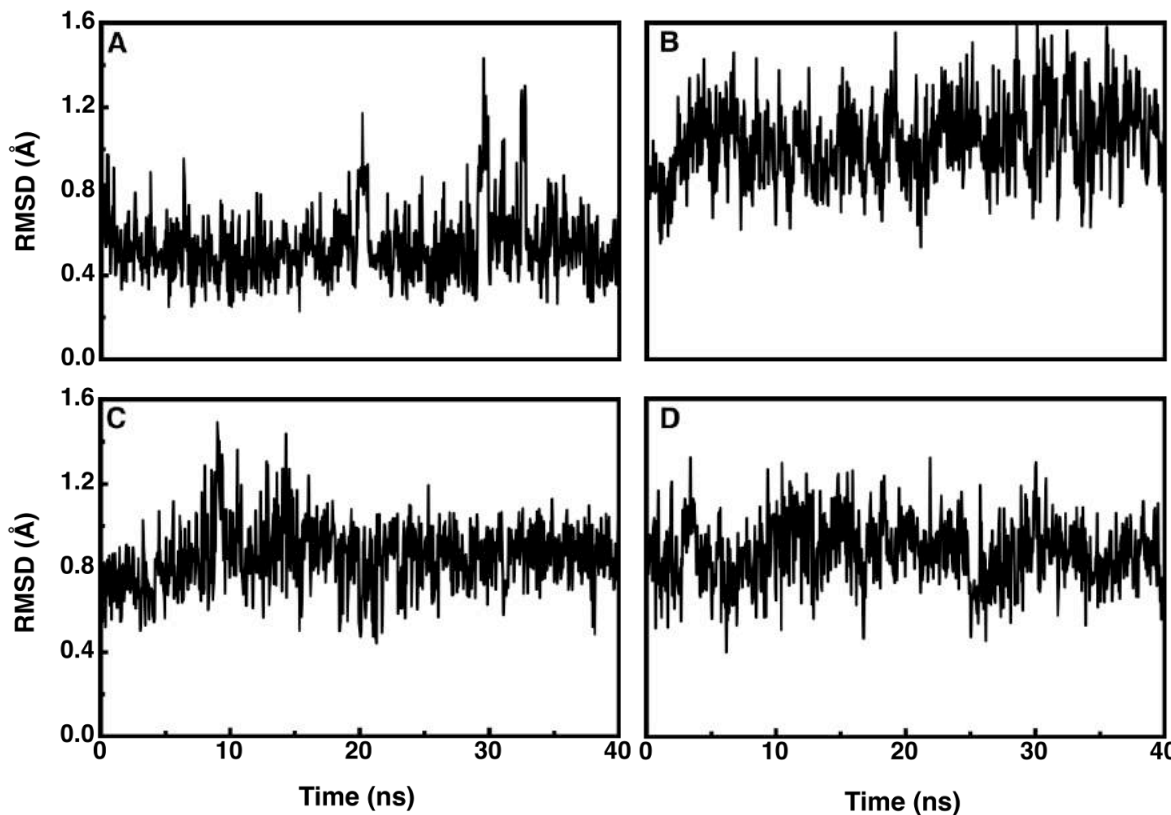


Figure S6: Key enzyme-substrate distances during the equilibration of wild-type StEH1 in complex with (A,B) (*R*)- and (C,D) (*S*)-SO bound in **Mode1** and **Mode2** respectively (for a definition of the two binding modes see **Figure 4** of the main text). RMSD plots are shown in Å, relative to the original crystal structure.

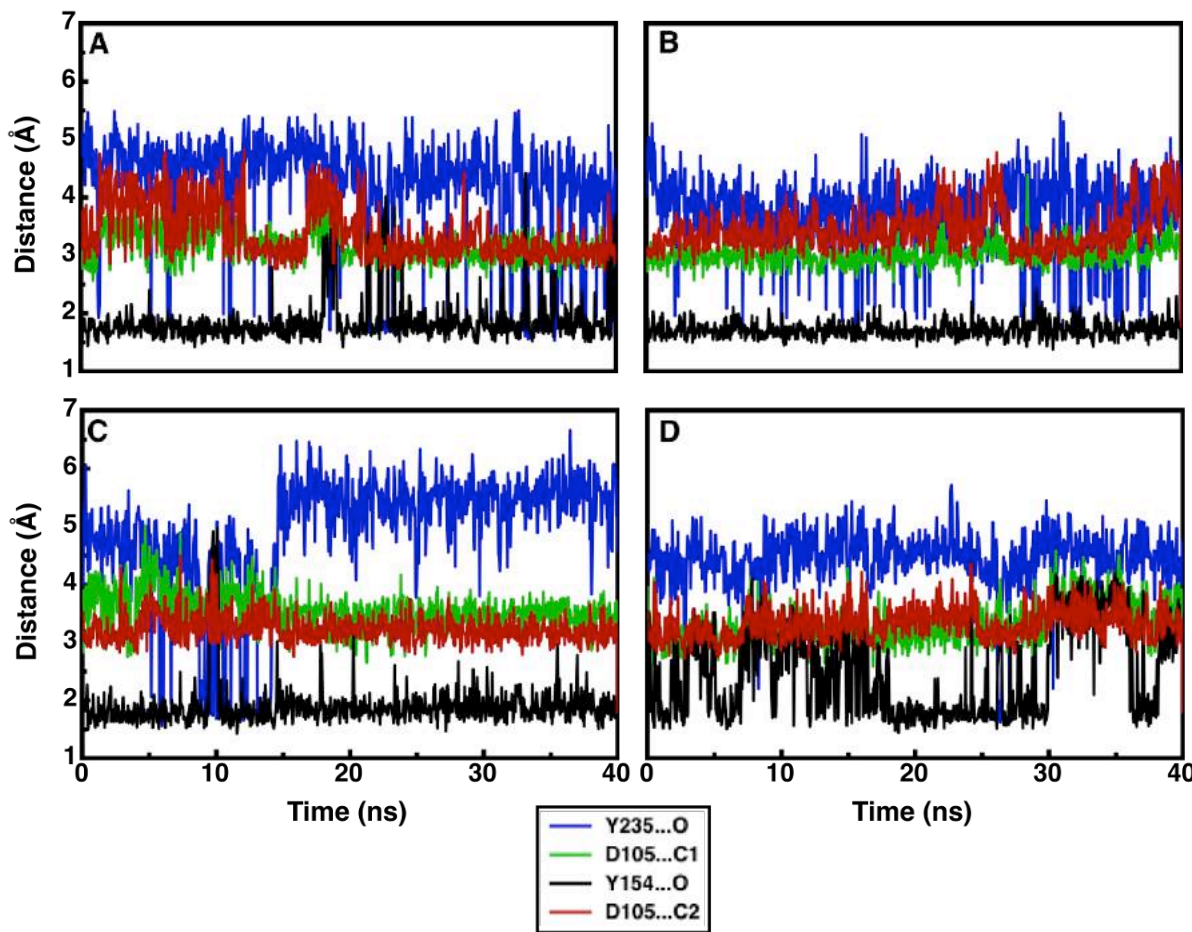


Figure S7: Key enzyme-substrate distances during the equilibration of the R-C1B1 variant of StEH1 in complex with **(A,B)** (*R*)- and **(C,D)** (*S*)-SO bound in **Mode1** and **Mode2** respectively (for a definition of the two binding modes see **Figure 4** of the main text). RMSD plots are shown in Å, relative to the original crystal structure.

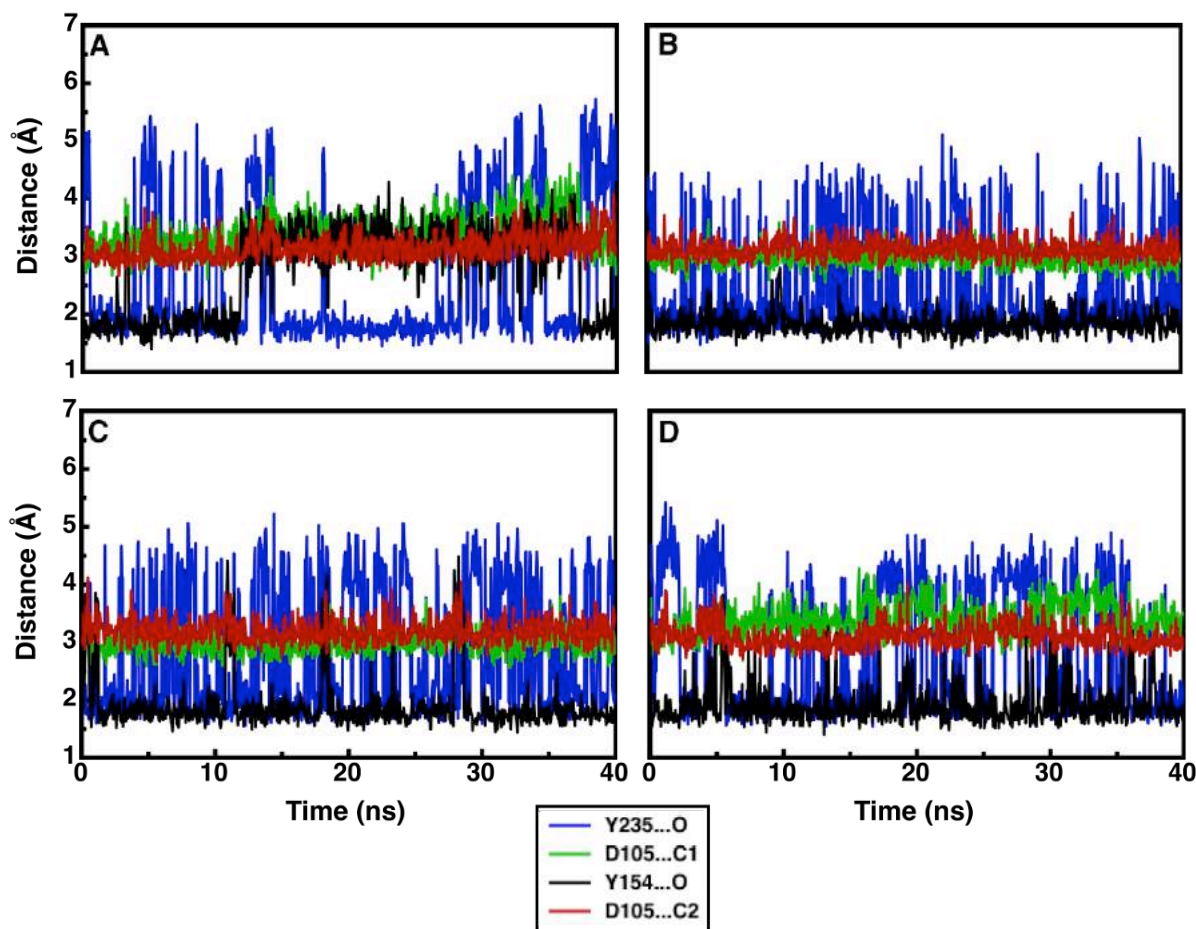


Figure S8: Representative structures of the transition state for the formation of the alkylenzyme intermediate, from our EVB simulations of wild-type StEH1 in complex with (A,B) (*R*)- and (C,D) (*S*)-SO, with the substrate placed in the active site in (A,C) **Mode 1** and (B,D) **Mode 2** respectively. The figure highlights the distances of the bonds that are being formed and broken at the transition state for each enantiomer and binding mode. The C-1 hydrogen has also been included in this figure to illustrate the stereochemistry. For discussion of the associated activation and reaction free energies for the different binding modes, see the main text.

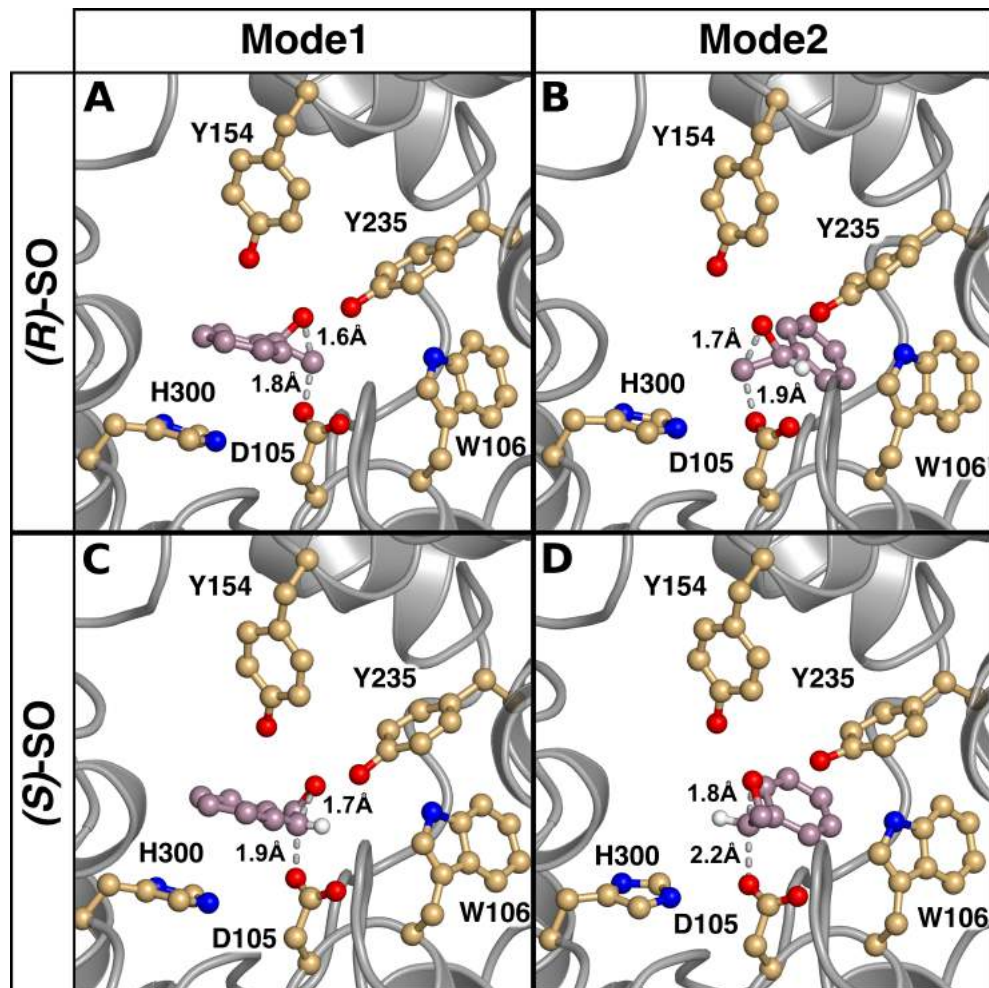


Figure S9: Representative structures of the alkylenzyme intermediates obtained from our EVB simulations of wild-type StEH1 in complex with (A,B) (*R*)- and (C,D) (*S*)-SO₂, with the substrate placed in the active site in (A,C) **Mode 1** and (B,D) **Mode 2** respectively. The C-1 hydrogen has been included in this figure to illustrate the stereochemistry. For discussion of the associated activation and reaction free energies for the different binding modes, see the main text.

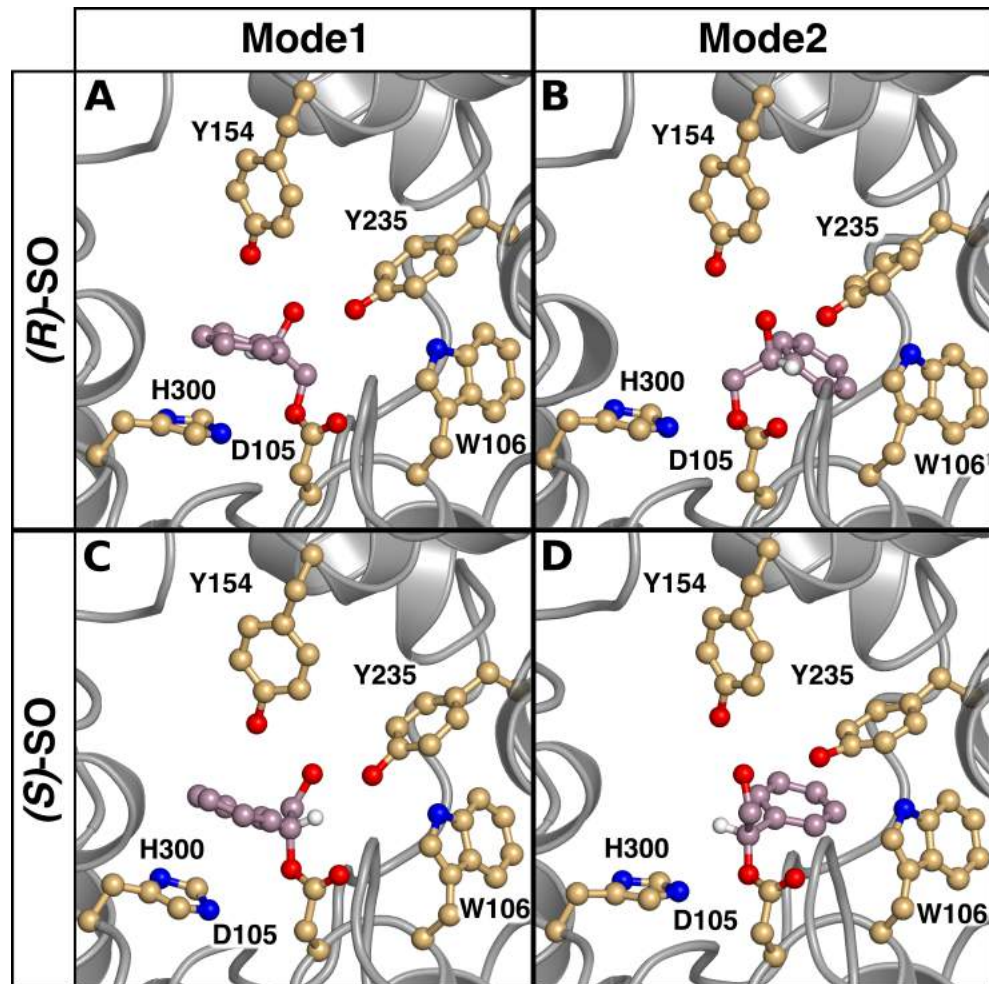


Figure S10: Representative structures of the transition state for the formation of the alkylenzyme intermediate, from our EVB simulations of R-C1B1 in complex with (A,B) (*R*)- and (C,D) (*S*)-SO, with the substrate placed in the active site in (A,C) **Mode 1** and (B,D) **Mode 2** respectively. The figure highlights the distances of the bonds that are being formed and broken at the transition state for each enantiomer and binding mode. The C-1 hydrogen has also been included in this figure to illustrate the stereochemistry. For discussion of the associated activation and reaction free energies for the different binding modes, see the main text.

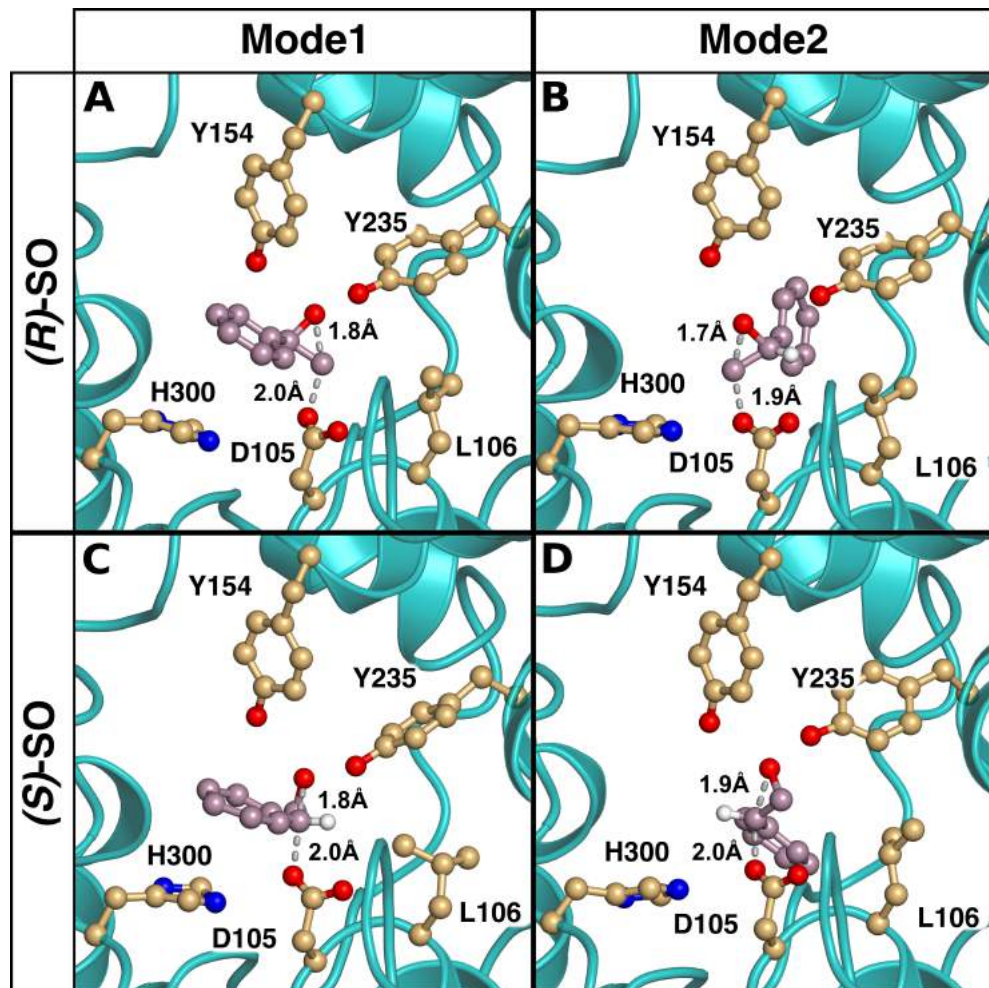


Figure S11: Representative structures of the alkylenzyme intermediate obtained from our EVB simulations of R-C1B1 in complex with (A,B) (*R*)- and (C,D) (*S*)-SO, with the substrate placed in the active site in (A,C) **Mode 1** and (B,D) **Mode 2** respectively. The C-1 hydrogen has been included in this figure to illustrate the stereochemistry. For discussion of the associated activation and reaction free energies for the different binding modes, see the main text.

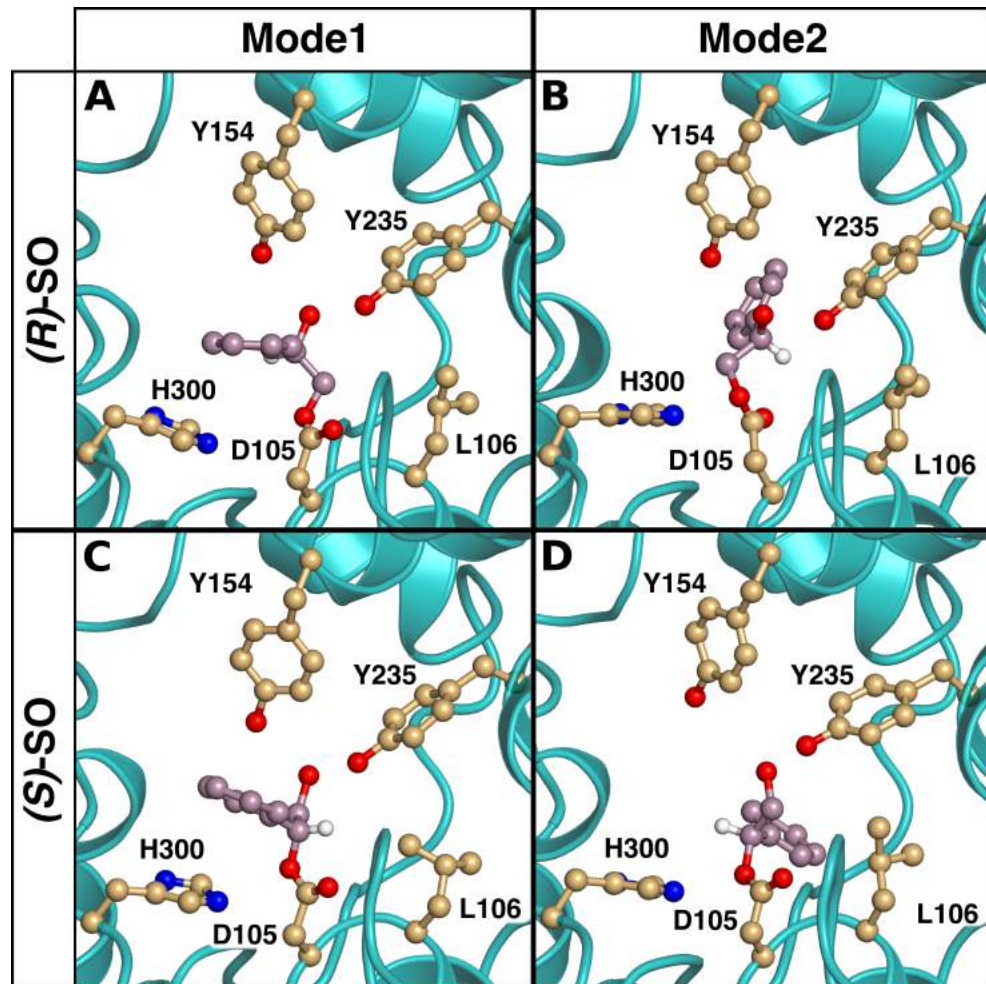


Table S1: A comparison of the energetics of the uncatalyzed hydrolysis of both (*R*)- and (*S*)-SO, from our DFT calculations and EVB calibration procedure^a. The corresponding absolute energies for the DFT calculations are shown in **Table S3**.

		(<i>R</i>)-SO		(<i>S</i>)-SO	
		C-1	C-2	C-1	C-2
<i>Ring Opening Step</i>					
DFT	ΔG^\ddagger	32.8	32.7	32.4	32.7
	ΔG_0	22.3	15.3	17.5	14.1
EVB	ΔG^\ddagger	32.8±0.1	32.7±0.1	32.4±0.2	32.7±0.1
	ΔG_0	22.3±0.1	15.3±0.1	17.5±0.2	14.1±0.1
<i>Hydrolysis Step</i>					
EVB	ΔG^\ddagger	19.0	19.0	19.0	19.0
	ΔG_0	10.0	10.0	10.0	10.0

^a DFT calculations performed as described in the main text and **Section S1**. In the second step, which involves ester hydrolysis by nucleophilic attack of a water molecule on an ester intermediate (**Figure 1** of main text), all EVB energetics were calibrated to a ΔG^\ddagger of 19 kcal mol⁻¹ and a ΔG_0 of 10 kcal mol⁻¹, as described in **Section S1** and the Supporting Information of our previous work¹. As the two binding modes described in **Figure 4** of the main text should have identical energetics in aqueous solution, we performed calculations for both SO conformations for each enantiomer, and used the conformation that gave the lowest calculated energetics (corresponding to **Mode2** for (*R*)-SO, **Mode1** for (*S*)-SO attack at C-1, and **Mode2** for (*S*)-SO attack at C-2) for all subsequent calibration. All energies provided in kcal mol⁻¹.

Table S2: Averages of key enzyme-substrate distances and susbtrate RMSD over our initial equilibration runs of either wild-type StEH1 or the R-C1B1 variant^a.

Variant	RMSD	Distances			
		Y154 - O	Y235 - O	D105 - C-1	D105 - C-2
(R)-SO					
Wild-type, Mode 1	0.58±0.20	2.74±0.76	2.57±1.25	3.39±0.35	3.15±0.22
Wild-type, Mode 2	1.00±0.17	1.84±0.19	2.41±0.89	2.98±0.17	3.13±0.17
R-C1B1, Mode 1	0.54±0.17	1.86±0.40	4.26±0.88	3.17±0.28	3.39±0.48
R-C1B1, Mode 2	1.04±0.20	1.72±0.14	3.75±0.68	3.01±0.18	3.43±0.37
(S)-SO					
Wild-type, Mode 1	0.85±0.14	1.89±0.45	2.82±1.13	2.98±0.18	3.19±0.21
Wild-type, Mode 2	0.87±0.20	1.92±0.35	2.88±1.15	3.41±0.29	3.11±0.20
R-C1B1, Mode 1	0.85±0.16	1.90±0.40	4.92±1.06	3.56±0.33	3.23±0.23
R-C1B1, Mode 2	1.09±0.20	2.47±0.76	4.43±0.49	3.33±0.36	3.33±0.28

^a All values are shown in Å, and are averages and standard deviations over 800 data points from 40 ns equilibration runs on each structure. Y154-O and Y235-O denote distances between the oxygen atoms of the tyrosine side chains and the epoxide ring oxygen, and D105-C-1 and D105-C-2 indicate distances between the nucleophilic oxygen atom of the D105 side chain and the relevant carbon atom of styrene oxide.

Table S3: Absolute electronic energy (E_{el} , in atomic units), zero-point energy contribution (E_{ZPE} , in $\text{kcal}\cdot\text{mol}^{-1}$), entropies (S , in $\text{cal}\cdot\text{mol}^{-1}\cdot\text{K}^{-1}$) and frequencies (ν , in cm^{-1}) for each optimized stationary point along the reaction profiles of nucleophilic attack of acetate on styrene oxide. RS, TS, and PS denote reactant, transition and product states respectively.

Species		E_e (a.u)	E_{ZPE} ($\text{kcal}\cdot\text{mol}^{-1}$)	S ($\text{cal}\cdot\text{mol}^{-1}\cdot\text{K}^{-1}$)	ν (cm^{-1})
(R)-SO					
RS		-652.9989558	134.518	157.478	
(R)-C-1 Mode1	TS	-652.9642824	134.580	118.272	-324.5
	PS	-652.9863124	136.274	115.047	52.1
(R)-C-1 Mode2	TS	-652.9655658	134.531	118.524	-346.9
	PS	-652.9933375	136.167	115.841	55.9
(R)-C-2 Mode1	TS	-652.9656463	134.622	118.546	-501.0
	PS	-652.9969483	136.361	116.548	41.1
(R)-C-2 Mode2	TS	-652.9652423	134.627	118.465	-498.7
	PS	-652.9969483	136.362	116.548	41.1
(S)-SO					
(S)-C-1 Mode1	TS	-652.9638628	134.568	118.208	-320.6
	PS	-652.9863124	136.274	115.047	52.1
(S)-C-1 Mode2	TS	-652.9658663	134.483	119.089	-353.3
	PS	-652.9933375	136.167	115.841	55.9
(S)-C-2 Mode1	TS	-652.9656463	134.622	118.546	-501.0
	PS	-652.9987326	136.453	117.166	42.2
(S)-C-2 Mode2	TS	-652.9656463	134.622	118.546	-501.0
	PS	-652.9969483	136.362	116.548	41.1

S4. Empirical Valence Bond Parameters Used in This Work

All relevant parameters to conduct the calculations were obtained as described in the Methodology section of the main text, with the standard amino acid and solvent parameters used as implemented in OPLS-AA. To construct the EVB Hamiltonian and obtain the free energy of a system, two additional parameters are needed. The first is a simple shift of the absolute energy to correct for differences in solvation free energy, referred to in the literature as the “gas phase shift” (α_i)²⁶⁻²⁸. The second parameter relates to the symmetric off-diagonal elements of the Hamiltonian, which are used to couple the two independent, diabatic states together in order to obtain the ground state free energy. The general function form is shown below:

$$H_{ij} = A_{ij} \exp[-\mu(r_{ij} - r_0)] \quad (2)$$

Here, r_{ij} denotes a specified reaction coordinate distance at the current simulation step (symbolizing wave function overlap), with r_0 as the equilibrium value, μ as a scaling term and A_{ij} a constant value that describes this reaction. In practice, the distance dependent part can be excluded due to limited changes in the overlap of the two state wave functions during the simulations. This limits the term to the constant A_{ij} and also prevents over-fitting the results. The two terms A_{ij} and (α_i) are subsequently changed to fit the calculated energy of the reference reaction to the relevant experimental or computational values. After this fitting is completed, the values are left unchanged for the energy calculations of the enzyme reactions. This means the fitting procedure is *only* used for the reference reactions.

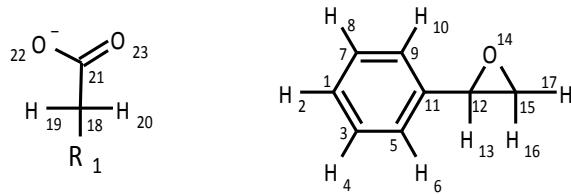
Table S4: EVB parameters used in this work^a.

Step I (Alkylation)				
	C-1		C-2	
	H_{ij}	α_i	H_{ij}	α_i
(R)-SO	68.76	-16.00	53.63	-14.06
(S)-SO	68.02	-24.27	59.30	-15.09
Step II (Hydrolysis)				
	C-1		C-2	
	H_{ij}	α_i	H_{ij}	α_i
(R)-SO	50.28	342.99	44.18	306.00
(S)-SO	44.43	326.32	48.14	301.58

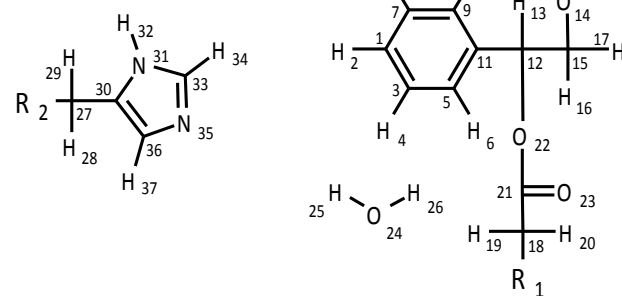
^a Both H_{ij} and α_i are constants. All values given in kcal mol⁻¹. Energy values were split over 100 sampling bins of equal width, with the first 1000 points (equal to 5 ps simulation time) of each data collection window being skipped as equilibration, and only bins with more than 250 points being considered as statistically significant.

Figure S12: Structures of the different VB states used in this work.

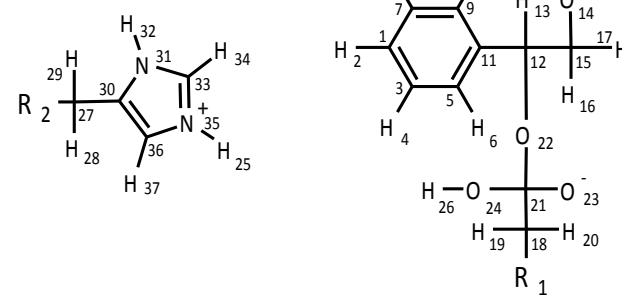
STATE I



STATE II



STATE III



EVB Parameters

Table S5: Van der Waals parameters used for atoms constituting the reacting system^a.

Type	A _i (kcal ^{1/2} ·mol ^{-1/2} ·Å ⁶)	B _i (kcal ^{1/2} ·mol ^{-1/2} ·Å ³)	C _i (kcal·mol ⁻¹)	α _i (Å ²)	A ₁₋₄ (kcal ^{1/2} ·mol ^{-1/2} ·Å ³)	B ₁₋₄ (kcal ^{1/2} ·mol ^{-1/2} ·Å ³)	mass (a.u.)
CA	1059.13	23.67	0	0.0	748.92	16.74	12.01
CO4	1802.24	34.18	250	1.7	1274.38	24.17	12.01
CT	944.52	22.03	250	2.5	667.88	15.58	12.01
CHMI	944.52	22.03	250	1.7	667.88	15.58	12.01
H	0.00	0.00	30	2.8	0.00	0.00	1.01
HA	69.58	4.91	0	0.0	49.20	3.47	1.01
HC	49.20	3.47	0	0.0	34.79	2.45	1.01
HC1	109.18	6.99	0	0.0	77.20	4.94	1.01
HC2	84.57	5.41	0	0.0	59.80	3.83	1.01
NA	971.75	28.31	180	2.5	687.13	20.02	14.01
O	616.44	23.77	90	2.2	435.89	16.81	16.00
OCRB	616.44	23.77	90	1.8	435.89	16.81	16.00
OH	976.93	31.26	90	2.0	690.79	22.10	16.00
OH1	690.37	23.86	0	0.0	488.17	16.87	16.00
OH2	760.65	25.04	100	2.8	537.86	17.71	16.00
OS	445.13	18.25	90	2.0	314.75	12.91	16.00
OS1	445.13	18.25	0	0.0	314.75	12.91	16.00
OT3	762.88	24.39	100	2.8	539.44	17.25	16.00

^a For all atoms except reacting atoms, a standard 6-12 Lennard Jones potential was used. In the case of the reacting atoms, which change bonding patterns between atoms *i* and *j*, an alternate function of the form: $V_{react} = C_i C_j \exp(-\alpha_i \alpha_j r_{ij})$ was used to prevent artificial repulsion between these atoms as bonding patterns change. r_{ij} denotes the distance (Å) between atoms *i* and *j*.

Table S6: Atom types in the different VB states.

Atom Number	C-1 Attack			C-2 Attack	
	State I	State II	State III	State II	State III
1	CA	CA	CA	CA	CA
2	HA	HA	HA	HA	HA
3	CA	CA	CA	CA	CA
4	HA	HA	HA	HA	HA
5	CA	CA	CA	CA	CA
6	HA	HA	HA	HA	HA
7	CA	CA	CA	CA	CA
8	HA	HA	HA	HA	HA
9	CA	CA	CA	CA	CA
10	HA	HA	HA	HA	HA
11	CA	CA	CA	CA	CA
12	CT	CT	CT	CT	CT
13	HC2	HC	HC	HC1	HC1
14	OS1	OH	OH	OH	OH
15	CT	CT	CT	CT	CT
16	HC2	HC1	HC1	HC	HC
17	HC2	HC1	HC1	HC	HC
18	CT	CT	CT	CT	CT
19	HC2	HC2	HC2	HC2	HC2
20	HC2	HC2	HC2	HC2	HC2
21	CO4	CO4	CHMI	CO4	CHMI
22	OCRB	OS	OS1	OS	OS1
23	O	O	OH	O	OH
24	OT3	OT3	OH2	OT3	OH2
25	H	H	H	H	H
26	H	H	H	H	H
27	CT	CT	CT	CT	CT
28	HC2	HC2	HC2	HC2	HC2
29	HC2	HC2	HC2	HC2	HC2
30	CA	CA	CA	CA	CA
31	NA	NA	NA	NA	NA
32	H	H	H	H	H
33	CA	CA	CA	CA	CA
34	HA	HA	HA	HA	HA
35	NA	NA	NA	NA	NA
36	CA	CA	CA	CA	CA
37	HA	HA	HA	HA	HA

Table S7: Partial charges of each atom in the reacting system.

#	(S)-SO						(R)-SO					
	C-1 Attack			C-2 Attack			C-1 Attack			C-2 Attack		
	State I	State II	State III	State II	State III	State I	State II	State III	State II	State III	State II	State III
1	-0.1365	-0.1246	-0.1451	-0.1530	-0.2027	-0.1365	-0.1291	-0.1886	-0.1535	-0.1942		
2	0.1374	0.1036	0.0797	0.1047	0.0877	0.1374	0.1075	0.0861	0.1049	0.0883		
3	-0.1603	-0.2183	-0.232	-0.2162	-0.1839	-0.1603	-0.2320	-0.2190	-0.2161	-0.1936		
4	0.1466	0.1212	0.0974	0.1164	0.0892	0.1466	0.1258	0.0990	0.1167	0.0902		
5	-0.1603	-0.2183	-0.232	-0.2162	-0.1839	-0.1603	-0.2320	-0.2190	-0.2161	-0.1936		
6	0.1466	0.1212	0.0974	0.1164	0.0892	0.1466	0.1258	0.0990	0.1167	0.0902		
7	-0.1627	-0.0974	-0.0887	-0.0943	-0.1527	-0.1627	-0.0655	-0.1355	-0.0949	-0.1197		
8	0.1309	0.132	0.1312	0.1015	0.1171	0.1309	0.1143	0.1366	0.1017	0.1123		
9	-0.1627	-0.0974	-0.0887	-0.0943	-0.1527	-0.1627	-0.0655	-0.1355	-0.0949	-0.1197		
10	0.1309	0.132	0.1312	0.1015	0.1171	0.1309	0.1143	0.1366	0.1017	0.1123		
11	0.1552	-0.0011	0.0065	0.0069	0.0605	0.1552	0.0103	0.1436	0.0073	-0.0155		
12	-0.0497	0.3494	0.3457	0.5108	0.5755	-0.0497	0.2664	0.1518	0.5111	0.6053		
13	0.1271	0.0041	-0.026	-0.1442	-0.1847	0.1271	0.0038	-0.0039	-0.1444	-0.1761		
14	-0.2727	-0.9046	-0.9933	-0.9108	-0.9882	-0.2727	-0.9162	-1.0192	-0.9109	-0.9981		
15	-0.1760	0.4449	0.5741	0.0783	0.1965	-0.1760	0.4367	0.5627	0.0746	0.2818		
16	0.1531	-0.1319	-0.1842	0.0468	-0.0322	0.1531	-0.1055	-0.1480	0.0480	-0.0598		
17	0.1531	-0.1319	-0.1842	0.0468	-0.0322	0.1531	-0.1055	-0.1480	0.0480	-0.0598		
18	-0.4798	-0.332	-0.8301	-0.3287	-0.7969	-0.4798	-0.1566	-0.8558	-0.3291	-0.8133		
19	0.0927	0.0919	0.1702	0.0984	0.1556	0.0927	0.0394	0.2062	0.0888	0.1629		
20	0.0927	0.1279	0.2113	0.0890	0.2018	0.0927	0.0545	0.2171	0.0984	0.1926		
21	0.9712	0.9206	1.3538	0.9852	1.2756	0.9712	0.7186	1.2699	0.9847	1.3502		
22	-0.8384	-0.6660	-0.809	-0.5803	-0.6934	-0.8384	-0.3500	-0.6678	-0.5782	-0.7461		
23	-0.8384	-0.6253	-0.9045	-0.6647	-0.9239	-0.8384	-0.5984	-0.8971	-0.6645	-0.9372		
24	-0.8340	-0.8340	-0.8351	-0.8340	-0.8187	-0.8340	-0.8340	-0.8160	-0.8340	-0.8478		
25	0.4170	0.4170	0.3544	0.4170	0.3803	0.4170	0.4170	0.3448	0.4170	0.3884		
26	0.4170	0.4170	0.4600	0.4170	0.4600	0.4170	0.4170	0.4600	0.4170	0.4600		
27	-0.0050	-0.0050	-0.0050	-0.0050	-0.0050	-0.0050	-0.0050	-0.0050	-0.0050	-0.0050		
28	0.0600	0.0600	0.0600	0.0600	0.0600	0.0600	0.0600	0.0600	0.0600	0.0600		
29	0.0600	0.0600	0.0600	0.0600	0.0600	0.0600	0.0600	0.0600	0.0600	0.0600		
30	0.0150	0.0150	0.2150	0.0150	0.2150	0.0150	0.0150	0.2150	0.0150	0.2150		
31	-0.5700	-0.5700	-0.5400	-0.5700	-0.5400	-0.5700	-0.5700	-0.5400	-0.5700	-0.5400		
32	0.4200	0.4200	0.4600	0.4200	0.4600	0.4200	0.4200	0.4600	0.4200	0.4600		
33	0.2950	0.2950	0.3850	0.2950	0.3850	0.2950	0.2950	0.3850	0.2950	0.3850		
34	0.1150	0.1150	0.1150	0.1150	0.1150	0.1150	0.1150	0.1150	0.1150	0.1150		
35	-0.4900	-0.4900	-0.5400	-0.4900	-0.5400	-0.4900	-0.4900	-0.5400	-0.4900	-0.5400		
36	-0.0150	-0.0150	0.2150	-0.0150	0.2150	-0.0150	-0.0150	0.2150	-0.0150	0.2150		
37	0.1150	0.1150	0.1150	0.1150	0.1150	0.1150	0.1150	0.1150	0.1150	0.1150		

Table S8: Bond parameters for the covalent bonds of the reacting system^a.

Bond Type	E_D (kcal·mol ⁻¹)	α (Å ⁻²)	r_0 (Å)	k_b (kcal·mol ⁻¹ ·Å ⁻²)	b (Å)
0	Not Set				
1				734	1.0800
2				938	1.4000
3				634	1.5100
4				680	1.0900
5				536	1.5290
6				640	1.4100
7				634	1.5220
8				428	1.3270
9				1140	1.2290
10				634	1.5040
11				854	1.3810
12				1040	1.3700
13				868	1.0100
14				954	1.3430
15				976	1.3350
16				820	1.3940
17				1312	1.2500
18				1106	0.9570
19				900	1.3640
20				1106	0.9450
21				560	1.5100
22				680	1.0880
23				520	1.5090
24				640	1.3800
25	80.00	2.0	1.4100		
26	80.00	2.0	1.3800		
27	284.7	1.2	1.0100		
28	245.8	1.5	0.9572		

^a Morse bonds (reacting atoms): $V_{\text{Morse}} = D_e \{1 - \exp[-\alpha (r_{ij} - r_0)]\}^2$; Harmonic bonds (non-reacting atoms): $V_{\text{Harmonic}} = 0.5k (r_{ij} - r_0)^2$.

Table S9: Bond types in different VB states.

Number		Bond Type				
		C-1 Attack		C-2 Attack		
#1	#2	State I	State II	State III	State II	State III
1	2			1		
1	3			2		
1	7			2		
3	4			1		
3	5			2		
5	6			1		
5	11			2		
7	8			1		
7	9			2		
9	10			1		
9	11			2		
11	12	21	3	3	3	3
12	13	22	4	4	4	4
12	14	6/25	0	0	6	6
12	15	23	5	5	5	5
12	22	0	25	6	0	0
14	15	6/25	6	6	0	0
15	16	22	4	4	4	4
15	17	22	4	4	4	4
15	22	0	0	0	25	6
18	19			4		
18	20			4		
18	21	7	7	5	7	5
21	22	17	8	24	8	24
21	23	17	9	24	9	24
21	24	0	0	26	0	26
24	25	18	28	0	28	0
24	26	18	18	20	18	20
27	28			4		
27	29			4		
27	30			10		
30	31			11		
30	36			12		
31	32			13		
31	33			14		
33	34			1		

33	35	15	15	14	15	14
35	25	0	0	27	0	27
35	36	16	16	11	16	11
36	37			1		
R₁	18			5		
R₂	27			5		

Table S10: Angle parameters used for bending adjacent bonds in the reacting system^a.

Angle Type	k_a (kcal·mol ⁻¹ ·rad ⁻²)	Θ_0 (°)	Angle Type	k_a (kcal·mol ⁻¹ ·rad ⁻²)	Θ_0 (°)		
0			No Set				
1	70.0	120.00	17	140.0	109.80		
2	126.0	120.00	18	140.0	110.00		
3	140.0	120.00	19	140.0	111.00		
4	70.0	109.50	20	70.0	128.20		
5	126.0	114.00	21	116.7	112.70		
6	100.0	109.50	22	140.0	117.00		
7	75.0	110.70	23	160.0	126.00		
8	66.0	107.80	24	200.0	104.52		
9	126.0	111.10	25	70.0	113.00		
10	162.0	111.40	26	75.0	117.20		
11	160.0	120.40	27	75.0	117.20		
12	166.0	123.40	28	60.0	60.00		
13	166.0	116.90	29	185.2	111.55		
14	140.0	121.60	30	120.0	109.50		
15	140.0	130.70	31	70.0	130.70		
16	140.0	106.30	32	110.0	108.50		
33	66.0	107.8	34	70	114.3		

^a Angle potential: $V_{\text{angle}} = 0.5 \sum k (\Theta - \Theta_0)^2$

Table S11: Angle types of the different VB states.

Atom Number			Angle Type				
#1	#2	#3	State I	State II	State III	State II	State III
1	3	4			1		
1	3	5			2		
1	7	8			1		
1	7	9			2		
2	1	3			1		
2	1	7			1		
3	1	7			2		
3	5	6			1		
3	5	11			2		
4	3	5			1		
5	11	9			2		
5	11	12			3		
6	5	11			1		
7	9	10			1		
7	9	11			2		
8	7	9			1		
9	11	12			3		
10	9	11			1		
11	12	13			4		
11	12	14	6	0	0	6	6
11	12	15			5		
11	12	22	0	6	6	0	0
12	14	15	28	0	0	0	0
12	15	14	28	6	6	0	0
12	15	16	27	7	7	7	7
12	15	17	27	7	7	7	7
12	15	22	0	0	0	6	6
13	12	14	26	0	0	4	4
12	22	21	0	13	30	0	0
13	12	15	27	7	7	7	7
13	12	22	0	4	4	0	0
14	12	15	28	0	0	6	6
14	15	16	26	4	4	0	0
14	15	17	26	4	4	0	0
15	12	22	0	6	6	0	0
15	22	21	0	0	0	13	30
16	15	17	34	33	33	33	33

16	15	22	0	0	0	4	4
17	15	22	0	0	0	4	4
18	21	22	22	10	6	10	6
18	21	23	22	11	6	11	6
18	21	24	0	0	6	0	6
19	18	20	8	8	8	8	8
19	18	21	4	4	7	4	7
20	18	21	4	4	7	4	7
21	24	26	0	0	32	0	32
22	21	23	23	12	29	12	29
22	21	24	0	0	29	0	29
23	21	24	0	0	29	0	29
25	24	26	24	24	0	24	0
27	30	31			14		
27	30	36			15		
28	27	29			8		
28	27	30			4		
29	27	30			4		
30	31	32			1		
30	31	33			17		
30	36	35	19	19	16	19	16
30	36	37	20	20	31	20	31
31	30	36			16		
31	33	34			1		
31	33	35			3		
32	31	33			1		
33	35	25	0	0	1	0	1
33	35	36	18	18	17	18	17
34	33	35			1		
35	36	37			1		
36	35	35	0	0	1	0	1
R ₁	18	19			7		
R ₁	18	20			7		
R ₁	18	21	9	9	21	9	21
R ₂	27	28			7		
R ₂	27	29			7		
R ₂	27	30			5		

Table S12: Torsion parameters used in the reacting system^a.

Torsion Type	V ₁	V ₂	V ₃	Torsion Type	V ₁	V ₂	V ₃	
	0.5·barrier height (kcal·mol ⁻¹)				0.5·barrier height (kcal·mol ⁻¹)			
0		Not Set		15	1.1830	-0.1310	0.2530	
1	0.0000	3.6250	0.0000	16	0.0000	0.0000	0.2100	
2	0.8550	-0.2500	0.3310	17	0.0000	1.4000	0.0000	
3	0.0000	0.0000	0.2310	18	0.0000	5.3750	0.0000	
4	-0.8485	-0.2280	0.2925	19	0.0000	2.3250	0.0000	
5	0.0000	0.0000	0.2340	20	0.0000	5.0000	0.0000	
6	0.0000	0.0000	0.1500	21	0.0000	2.4000	0.0000	
7	2.1590	0.0000	0.0000	22	0.0000	0.4100	0.0000	
8	-0.6100	-0.0630	0.2110	23	0.3250	-0.1250	0.3350	
9	0.0000	0.0000	0.0990	24	0.0000	0.0000	0.3800	
10	0.0000	0.0000	-0.2760	25	-0.6680	0.0000	0.0000	
11	-0.1390	0.6140	-0.3470	26	-0.2610	-1.0090	0.9980	
12	0.0000	0.0000	0.0660	27	-0.1780	-0.0870	0.2460	
13	2.3350	2.5620	0.0000	28	-0.6280	-0.9030	0.0020	
14	0.0000	2.5620	0.0000	29	0.0000	1.6000	0.0000	

^a Torsion angle potential: $V_{\text{torsion}} = V_1 (1+\cos(n\varphi -\delta))+ V_2 (1+\cos2(n\varphi -\delta))+ V_3 (1+\cos3(n\varphi -\delta))$, n is the periodicity (number of maxima per turn) and δ is the phase shift.

Table S13: Torsion types in the different VB states.

Atom Number				Torsion Type				
#1	#2	#3	#4	State I	State II	State III	State II	State III
1	3	5	6				1	
1	3	5	11				1	
1	7	9	10				1	
1	7	9	11				1	
2	1	3	4				1	
2	1	3	5				1	
2	1	7	8				1	
2	1	7	9				1	
3	1	7	8				1	
3	1	7	9				1	
3	5	11	9				1	
3	5	11	12				1	
4	3	5	6				1	
4	3	5	11				1	
6	5	11	9				1	
6	5	11	12				1	
7	1	3	4				1	
7	1	3	5				1	
7	9	11	5				1	
7	9	11	12				1	
8	7	9	10				1	
8	7	9	11				1	
10	9	11	5				1	
10	9	11	12				1	
11	12	14	15	23	0	0	0	0
11	12	15	14	2	2	2	0	0
11	12	15	16			3		
11	12	15	17			3		
11	12	15	22	0	0	0	2	2
11	12	22	21	0	7	23	0	0
12	14	15	16	24	0	0	0	0
12	14	15	17	24	0	0	0	0
12	15	22	21	0	0	0	8	23
13	12	14	15	24	0	0	0	0
13	12	15	14	5	5	5	0	0
13	12	15	16			6		
13	12	15	17			6		
13	12	15	22	0	0	0	5	5

13	12	22	21	0	9	24	0	0
14	12	15	16	5	0	0	5	5
14	12	15	17	5	0	0	5	5
14	12	15	22	0	0	0	7	7
15	12	22	21	0	8	23	0	0
16	15	22	21	0	0	0	9	24
17	15	22	21	0	0	0	9	24
18	21	22	12	0	13	23	0	0
18	21	22	15	0	0	0	13	23
18	21	24	26	0	0	27	0	27
19	18	21	22	0	12	5	12	5
19	18	21	23	0	0	5	0	5
19	18	21	24	0	0	5	0	5
20	18	21	22	0	12	5	12	5
20	28	11	23	0	0	5	0	5
20	18	21	24	0	0	5	0	5
22	12	15	14	0	7	7	0	0
22	12	15	16	0	5	5	0	0
22	12	15	17	0	5	5	0	0
22	21	24	26	0	0	28	0	28
23	21	22	12	0	14	26	0	0
23	21	22	15	0	0	0	14	26
23	21	24	26	0	0	28	0	28
24	21	22	12	0	0	26	0	0
24	21	22	15	0	0	0	0	26
25	35	36	30	0	0	17	0	17
25	35	36	37	0	0	29	0	29
27	30	31	32			17		
27	30	31	33			17		
27	30	36	35			18		
27	30	36	37			18		
28	27	30	31			16		
29	27	30	31			16		
30	31	33	34			19		
30	31	33	35			19		
31	30	36	35			18		
31	30	36	37			18		
31	33	35	36	20	20	19	20	19
31	33	35	25	0	0	19	0	19
32	31	33	34			19		
32	31	33	35			19		
33	35	36	30	21	21	17	21	21
33	35	36	37	21	21	29	21	29

34	33	35	36	20	20	19	20	19
34	33	35	25	0	0	19	0	19
36	30	31	32			17		
36	30	31	33			17		
R₁	18	21	22	22	10	25	20	25
R₁	18	21	23	22	11	25	11	25
R₁	18	21	24	0	0	25	0	25
R₂	27	30	31			15		

Table S14: Improper torsion parameters in the reacting system^a.

Improper Type	k_a (kcal·mol ⁻¹ rad ⁻²)	τ_0 (°)
0		Not Set
1	1.1	180
2	10.5	180
3	1.0	180

^a Improper torsion potential: $V_{\text{torsion}} = k (\tau - \tau_0)^2$.. k_i is the force constant and τ is the equilibrium angle (in degrees).

Table S15: Improper torsion angles of the different VB states.

#1	#2	#3	#4	Improper Type		
				State I	State II	State III
1	3	5	4		1	
1	7	9	8		1	
3	1	7	2		1	
11	5	3	6		1	
11	9	7	10		1	
12	11	5	9		1	
18	21	22	23	2	2	0
27	30	36	31		1	
30	31	33	32		3	
30	36	37	35		1	
33	35	36	25	0	0	3
34	33	31	35		1	

S5. Cartesian Coordinates for Key Stationary Points

Optimized stationary points along the reaction profiles of the nucleophilic attack of propionate on (*S*)-SO and (*R*)-SO in all previously mentioned reaction pathways. RS, TS, and PS denote reactant, transition and product states respectively. The reactant state molecules are only shown once at infinite separation.

Reactant

Propionate

C	0.688639	0.050622	0.002436
C	-0.641637	-0.730274	0.026926
O	0.662131	1.317503	0.011174
O	1.747959	-0.653593	-0.020792
C	-1.924175	0.102486	-0.019968
H	-0.629343	-1.353937	0.932048
H	-0.617243	-1.436619	-0.814176
H	-1.991181	0.783670	0.836151
H	-2.806125	-0.550279	-0.001385
H	-1.973789	0.708881	-0.932064

Styreneoxide

H	-0.416561	1.878560	-0.066467
C	0.302392	1.064126	-0.031337
C	1.669874	1.347690	0.004302
H	2.005239	2.381936	0.001877
C	2.606576	0.306772	0.041492
H	3.670144	0.530140	0.069240
C	2.166271	-1.020621	0.036722
H	2.885524	-1.835572	0.058876
C	0.797037	-1.304443	-0.006113
H	0.457499	-2.338058	-0.019255
C	-0.146631	-0.266596	-0.032647
C	-1.598738	-0.610619	-0.058277
C	-2.623592	0.141978	0.688818
O	-2.496370	0.305592	-0.739579
H	-1.813912	-1.657208	-0.271982
H	-2.324691	1.010729	1.273579
H	-3.531419	-0.364983	1.013001

(R)-SO C-1 Model

TS

C	-2.943337	-2.062500	0.317591
H	-3.555274	-2.935528	0.530161
C	-2.428189	-1.293355	1.369393
H	-2.640145	-1.568953	2.399374
C	-2.669509	-1.701648	-1.006790
H	-3.068636	-2.291750	-1.827790

C	-1.640902	-0.173090	1.101675
H	-1.247686	0.413133	1.926534
C	-1.885534	-0.577981	-1.274281
H	-1.674505	-0.296294	-2.303357
C	-1.358069	0.200769	-0.226225
C	-0.516295	1.357788	-0.559502
H	-0.460900	1.613604	-1.609313
O	-1.525795	3.018655	0.032072
C	-0.271978	2.490913	0.354819
H	-0.145928	2.217317	1.413056
H	0.588007	3.109081	0.048636
O	1.304772	0.382046	-0.968997
C	2.141609	-0.020898	-0.076511
O	2.035444	0.162519	1.157853
C	3.346688	-0.788108	-0.649655
H	2.947573	-1.651218	-1.199699
H	3.812984	-0.145049	-1.407900
C	4.385944	-1.244911	0.375702
H	5.201369	-1.781201	-0.125016
H	3.944588	-1.917756	1.119525
H	4.820620	-0.393028	0.911080

Product

C	-3.140031	-1.756841	0.322610
H	-3.908103	-2.486301	0.568196
C	-2.801821	-0.753919	1.237317
H	-3.307346	-0.700537	2.198724
C	-2.486859	-1.809367	-0.914318
H	-2.745903	-2.579123	-1.637507
C	-1.811939	0.184458	0.923603
H	-1.561265	0.954622	1.646001
C	-1.506099	-0.863420	-1.226369
H	-1.010737	-0.903319	-2.194569
C	-1.146070	0.139184	-0.309572
C	-0.068532	1.137541	-0.706561
H	-0.285318	1.486673	-1.720431
O	-0.944362	3.289356	-0.016971
C	0.104260	2.408075	0.161394
H	0.239018	2.101820	1.218490
H	1.089425	2.829716	-0.147547
O	1.223452	0.434074	-0.946162
C	1.899428	-0.170915	0.041179
O	1.543623	-0.196602	1.211331
C	3.158035	-0.830760	-0.492421
H	2.840461	-1.602714	-1.206463
H	3.702418	-0.083934	-1.083656
C	4.051815	-1.430292	0.592966
H	4.934672	-1.889349	0.134734
H	3.524002	-2.201949	1.163465
H	4.393850	-0.662695	1.295996

(R)-SO C-1 Mode2**TS**

C	3.470972	-1.687720	1.245923
H	3.356909	-0.995662	2.088001
H	4.376023	-2.283003	1.419113
H	2.612910	-2.369254	1.253676
C	3.579400	-0.938610	-0.083514
H	3.729552	-1.647691	-0.909196
H	4.466629	-0.291057	-0.085686
C	2.386809	-0.051402	-0.480161
O	1.381293	-0.026241	0.314578
O	2.472843	0.588989	-1.560580
C	-3.280230	-1.763212	-0.036468
H	-4.046527	-2.533622	-0.003924
C	-2.966834	-1.035641	1.119157
H	-3.489598	-1.241417	2.049813
C	-2.604168	-1.494492	-1.232388
H	-2.843153	-2.054481	-2.132912
C	-1.983664	-0.046042	1.081973
H	-1.750684	0.510361	1.985004
C	-1.622701	-0.502405	-1.269781
H	-1.097569	-0.292894	-2.198896
C	-1.299046	0.235946	-0.115607
C	-0.239200	1.249253	-0.197018
H	0.196993	1.415950	-1.172458
O	-1.121321	3.036219	0.062279
C	-0.098227	2.368527	0.747693
H	-0.322175	2.131519	1.799737
H	0.889493	2.854310	0.698659

Product

C	-4.605296	-1.201170	0.123485
H	-4.578350	-1.486538	1.180707
H	-5.208989	-1.941057	-0.413240
H	-5.107854	-0.230930	0.046033
C	-3.199955	-1.149313	-0.474978
H	-3.236410	-0.893146	-1.541769
H	-2.713995	-2.132269	-0.421396
C	-2.278689	-0.151709	0.198773
O	-1.062946	-0.156028	-0.371003
O	-2.588343	0.562146	1.144208
C	3.767815	-1.313930	0.072880
H	4.725126	-1.829332	0.059610
C	3.329638	-0.671618	1.234975
H	3.944506	-0.684777	2.131810
C	2.964070	-1.291306	-1.074353
H	3.296664	-1.789928	-1.981782
C	2.092847	-0.015233	1.249233
H	1.752431	0.474877	2.158871
C	1.735050	-0.626258	-1.059046

H	1.121517	-0.611296	-1.956391
C	1.283324	0.018962	0.104712
C	-0.027397	0.768453	0.125058
H	-0.285221	1.042821	1.149991
O	0.799245	3.031252	-0.309091
C	-0.051627	2.050533	-0.759089
H	0.169581	1.711124	-1.798987
H	-1.121321	2.367033	-0.776276

(R)-SO C-2 Model1

TS

C	3.559831	-1.752469	-0.454651
H	4.217620	-2.571345	-0.735049
C	3.193653	-1.569807	0.882217
H	3.567416	-2.245139	1.648009
C	3.077838	-0.871013	-1.430661
H	3.360400	-1.005608	-2.471996
C	2.349581	-0.511493	1.238199
H	2.071808	-0.368501	2.280620
C	2.234304	0.183234	-1.071398
H	1.869437	0.865535	-1.835247
C	1.857526	0.372503	0.267881
C	0.949389	1.512041	0.675982
H	0.889914	1.564761	1.771477
O	1.189955	2.764621	0.062197
C	-0.347022	1.664297	0.005261
H	-0.402664	1.468242	-1.055911
H	-1.076140	2.326346	0.448277
O	-1.471450	0.022811	0.462864
C	-2.655209	-0.037858	-0.045958
O	-3.147833	0.837610	-0.802309
C	-3.453837	-1.290278	0.324361
H	-2.918566	-2.147173	-0.107631
H	-3.386272	-1.415356	1.412355
C	-4.913650	-1.293923	-0.127496
H	-5.404850	-2.220316	0.193838
H	-4.999113	-1.229910	-1.217935
H	-5.468788	-0.453267	0.304756

Product

C	-3.369231	-1.790512	0.402668
H	-4.024894	-2.624058	0.643620
C	-3.019381	-1.527307	-0.925197
H	-3.403973	-2.155632	-1.725873
C	-2.867841	-0.968050	1.421552
H	-3.132339	-1.165290	2.458416
C	-2.172666	-0.451863	-1.227418
H	-1.905365	-0.253772	-2.264551
C	-2.028401	0.105295	1.110254
H	-1.655913	0.740897	1.911139

C	-1.664193	0.380590	-0.219736
C	-0.788744	1.595299	-0.569098
H	-0.594148	1.518984	-1.663744
O	-1.381012	2.797191	-0.223486
C	0.594937	1.504009	0.105538
H	0.507435	1.476085	1.196158
H	1.201020	2.366885	-0.184828
O	1.280541	0.290378	-0.338684
C	2.522168	0.061208	0.110103
O	3.107254	0.811493	0.881651
C	3.088586	-1.225154	-0.455900
H	2.406601	-2.036569	-0.169418
H	3.026953	-1.157433	-1.549808
C	4.517466	-1.528226	-0.006097
H	4.855605	-2.467919	-0.456228
H	4.579919	-1.630525	1.082648
H	5.208637	-0.735886	-0.313407

(R)-SO C-2 Mode2

TS

C	-3.067807	-2.351592	0.430611
H	-3.777125	-3.188360	0.421062
H	-2.801194	-2.147661	1.473768
H	-2.159451	-2.673600	-0.090833
C	-3.691531	-1.124651	-0.237305
H	-4.620356	-0.841275	0.276300
H	-3.985512	-1.359874	-1.269289
C	-2.824119	0.141689	-0.305757
O	-1.646714	0.076065	0.202467
O	-3.316379	1.161646	-0.851703
C	3.406184	-1.621299	-0.597887
H	4.073664	-2.399800	-0.959534
C	3.057577	-0.549213	-1.429914
H	3.454525	-0.494456	-2.441080
C	2.894627	-1.679951	0.702573
H	3.164469	-2.503861	1.359240
C	2.202308	0.453609	-0.964124
H	1.942818	1.286976	-1.612469
C	2.039072	-0.672423	1.164448
H	1.648429	-0.719095	2.179536
C	1.677717	0.400469	0.337039
C	0.745853	1.477988	0.854509
H	0.600000	1.345540	1.937363
O	1.032914	2.801886	0.475589
C	-0.501094	1.743722	0.123108
H	-0.471123	1.730275	-0.956789
H	-1.260439	2.338332	0.608099

Product

C	4.517475	-1.528220	-0.006099
H	4.855614	-2.467915	-0.456225
H	4.579937	-1.630510	1.082647
H	5.208640	-0.735879	-0.313420
C	3.088590	-1.225159	-0.455891
H	2.406610	-2.036574	-0.169397
H	3.026946	-1.157447	-1.549800
C	2.522170	0.061205	0.110106
O	1.280542	0.290370	-0.338679
O	3.107257	0.811496	0.881648
C	-3.369240	-1.790506	0.402669
H	-4.024906	-2.624049	0.643622
C	-2.867852	-0.968041	1.421552
H	-3.132354	-1.165276	2.458415
C	-3.019385	-1.527308	-0.925195
H	-3.403975	-2.155635	-1.725870
C	-2.028408	0.105301	1.110252
H	-1.655922	0.740906	1.911136
C	-2.172666	-0.451867	-1.227418
H	-1.905361	-0.253780	-2.264550
C	-1.664195	0.380590	-0.219737
C	-0.788742	1.595295	-0.569101
H	-0.594144	1.518976	-1.663747
O	-1.381005	2.797190	-0.223493
C	0.594938	1.504004	0.105538
H	0.507434	1.476083	1.196158
H	1.201024	2.366878	-0.184829

(S)-SO C-1 Mode1**TS**

C	-3.865883	-1.394006	-0.895187
H	-4.795340	-1.971360	-0.815830
H	-3.103668	-2.042013	-1.342187
H	-4.044333	-0.561442	-1.585251
C	-3.436575	-0.893750	0.485377
H	-3.293689	-1.741742	1.169382
H	-4.231434	-0.283040	0.934182
C	-2.146868	-0.055872	0.554327
O	-1.505352	0.114550	-0.543331
O	-1.808814	0.398784	1.675996
C	3.080075	-1.860160	0.365686
H	3.784609	-2.645999	0.626297
C	2.548425	-1.793544	-0.927393
H	2.838882	-2.525963	-1.676207
C	2.703379	-0.909267	1.323429
H	3.115291	-0.956672	2.328302
C	1.646497	-0.780574	-1.257841
H	1.235227	-0.726832	-2.263256

C	1.798580	0.100206	0.994060
H	1.514595	0.830235	1.745806
C	1.256850	0.178815	-0.303543
C	0.286918	1.211391	-0.692988
H	0.024784	1.239885	-1.742419
O	1.257276	2.998875	-0.653344
C	0.129445	2.501530	0.007852
H	0.222875	2.449663	1.102505
H	-0.817739	3.009005	-0.238581

Product

C	-4.051811	-1.430309	0.592956
H	-4.934669	-1.889360	0.134721
H	-4.393844	-0.662724	1.296000
H	-3.523992	-2.201973	1.163440
C	-3.158039	-0.830757	-0.492427
H	-3.702427	-0.083923	-1.083647
H	-2.840467	-1.602698	-1.206483
C	-1.899432	-0.170914	0.041177
O	-1.223451	0.434071	-0.946163
O	-1.543631	-0.196600	1.211330
C	3.140038	-1.756835	0.322610
H	3.908112	-2.486293	0.568194
C	2.486883	-1.809346	-0.914327
H	2.745943	-2.579088	-1.637525
C	2.801808	-0.753930	1.237328
H	3.307319	-0.700559	2.198743
C	1.506120	-0.863402	-1.226377
H	1.010773	-0.903289	-2.194585
C	1.811923	0.184445	0.923615
H	1.561234	0.954595	1.646022
C	1.146071	0.139186	-0.309570
C	0.068531	1.137540	-0.706558
H	0.285317	1.486675	-1.720427
O	0.944356	3.289355	-0.016962
C	-0.104265	2.408072	0.161398
H	-0.239026	2.101815	1.218493
H	-1.089430	2.829712	-0.147544

(S)-SO C-1 Mode2

TS

C	-3.500522	-1.715749	-0.109958
H	-4.302527	-2.442522	-0.212105
C	-2.698194	-1.710994	1.037140
H	-2.874309	-2.433359	1.830131
C	-3.267357	-0.780119	-1.126390
H	-3.888004	-0.780478	-2.018908
C	-1.671329	-0.773889	1.164968
H	-1.048260	-0.769283	2.056482

C	-2.238727	0.154408	-0.999441
H	-2.068824	0.874178	-1.794664
C	-1.427345	0.171563	0.150856
C	-0.319228	1.120636	0.318390
H	0.213307	1.083075	1.258614
O	-1.139213	2.938642	0.492930
C	-0.213479	2.394774	-0.407859
H	-0.545879	2.371418	-1.457505
H	0.794131	2.837624	-0.365249
O	1.186603	-0.087958	-0.585673
C	2.324187	-0.179481	0.008247
O	2.598454	0.321962	1.125443
C	3.381466	-0.986032	-0.766127
C	4.759890	-1.076029	-0.108971
H	2.967752	-1.991309	-0.924770
H	3.462485	-0.539495	-1.766133
H	5.440482	-1.664956	-0.736002
H	4.704400	-1.557723	0.873798
H	5.202311	-0.082876	0.029582

Product

C	-3.767811	-1.313936	0.072871
H	-4.725120	-1.829342	0.059597
C	-2.964076	-1.291280	-1.074369
H	-3.296676	-1.789881	-1.981807
C	-3.329625	-0.671650	1.234978
H	-3.944486	-0.684833	2.131818
C	-1.735059	-0.626227	-1.059056
H	-1.121534	-0.611241	-1.956407
C	-2.092838	-0.015260	1.249241
H	-1.752415	0.474830	2.158887
C	-1.283325	0.018966	0.104714
C	0.027396	0.768458	0.125065
H	0.285221	1.042816	1.150000
O	-0.799237	3.031264	-0.309066
C	0.051631	2.050546	-0.759072
H	-0.169577	1.711146	-1.798973
H	1.121327	2.367040	-0.776255
O	1.062943	-0.156022	-0.371006
C	2.278686	-0.151712	0.198770
O	2.588344	0.562134	1.144211
C	3.199947	-1.149317	-0.474987
C	4.605289	-1.201180	0.123473
H	2.713984	-2.132271	-0.421407
H	3.236400	-0.893147	-1.541777
H	5.208979	-1.941068	-0.413258
H	4.578344	-1.486553	1.180693
H	5.107850	-0.230942	0.046023

(S)-SO C-2 Mode1**TS**

C	-3.581867	-1.741662	-0.457878
H	-4.243579	-2.555745	-0.743877
C	-3.144301	-1.620915	0.865080
H	-3.466292	-2.339932	1.614848
C	-3.166064	-0.803160	-1.411535
H	-3.505074	-0.887892	-2.441537
C	-2.295791	-0.568157	1.228547
H	-1.962646	-0.475113	2.260788
C	-2.317764	0.245209	-1.043678
H	-2.005544	0.973901	-1.787721
C	-1.867728	0.371888	0.280135
C	-0.942557	1.498975	0.692529
H	-0.857076	1.520354	1.789485
O	-1.176858	2.760751	0.114162
C	0.344660	1.645329	-0.000543
H	0.371985	1.477904	-1.067359
H	1.092027	2.288190	0.439088
O	1.456217	-0.016355	0.369534
C	2.673579	-0.020776	-0.052816
O	3.212909	0.911623	-0.694071
C	3.459742	-1.295689	0.291276
H	3.407498	-1.425373	1.380624
H	2.904255	-2.142906	-0.133317
C	4.914638	-1.323631	-0.179753
H	5.389271	-2.268333	0.112124
H	5.493617	-0.504268	0.261419
H	4.984131	-1.233409	-1.269764

Product

C	3.369233	-1.790510	0.402670
H	4.024896	-2.624055	0.643625
C	3.019373	-1.527317	-0.925194
H	3.403957	-2.155649	-1.725867
C	2.867852	-0.968039	1.421552
H	3.132358	-1.165270	2.458415
C	2.172656	-0.451874	-1.227418
H	1.905348	-0.253791	-2.264550
C	2.028411	0.105306	1.110251
H	1.655931	0.740916	1.911133
C	1.664193	0.380589	-0.219739
C	0.788744	1.595297	-0.569103
H	0.594147	1.518979	-1.663749
O	1.381011	2.797189	-0.223493
C	-0.594937	1.504008	0.105535
H	-0.507433	1.476087	1.196155
H	-1.201021	2.366883	-0.184833
O	-1.280541	0.290376	-0.338682

C	-2.522169	0.061209	0.110105
O	-3.107254	0.811497	0.881650
C	-3.088588	-1.225154	-0.455895
H	-3.026958	-1.157433	-1.549804
H	-2.406602	-2.036569	-0.169415
C	-4.517467	-1.528225	-0.006089
H	-4.855607	-2.467919	-0.456218
H	-5.208639	-0.735886	-0.313397
H	-4.579917	-1.630523	1.082657

(S)-SO C-2 Mode2

TS

C	4.914646	-1.323622	-0.179746
H	4.984158	-1.233378	-1.269755
H	5.389278	-2.268328	0.112120
H	5.493614	-0.504265	0.261453
C	3.459742	-1.295696	0.291258
H	3.407479	-1.425404	1.380602
H	2.904266	-2.142906	-0.133364
C	2.673580	-0.020778	-0.052821
O	1.456216	-0.016363	0.369525
O	3.212911	0.911628	-0.694064
C	-3.581873	-1.741656	-0.457879
H	-4.243588	-2.555737	-0.743879
C	-3.144297	-1.620920	0.865077
H	-3.466282	-2.339943	1.614842
C	-3.166078	-0.803147	-1.411532
H	-3.505096	-0.887871	-2.441532
C	-2.295784	-0.568165	1.228546
H	-1.962631	-0.475129	2.260785
C	-2.317775	0.245219	-1.043674
H	-2.005562	0.973916	-1.787713
C	-1.867729	0.371887	0.280137
C	-0.942555	1.498971	0.692533
H	-0.857071	1.520346	1.789489
O	-1.176853	2.760749	0.114172
C	0.344661	1.645325	-0.000541
H	0.371984	1.477904	-1.067358
H	1.092030	2.288182	0.439092

Product

C	-4.517474	-1.528221	-0.006100
H	-4.579936	-1.630513	1.082645
H	-4.855612	-2.467915	-0.456228
H	-5.208640	-0.735880	-0.313420
C	-3.088589	-1.225158	-0.455893
H	-3.026946	-1.157444	-1.549801
H	-2.406609	-2.036573	-0.169400
C	-2.522170	0.061206	0.110107

O	-1.280543	0.290373	-0.338679
O	-3.107256	0.811495	0.881651
C	3.369240	-1.790505	0.402669
H	4.024905	-2.624049	0.643623
C	3.019384	-1.527308	-0.925195
H	3.403975	-2.155635	-1.725869
C	2.867851	-0.968041	1.421552
H	3.132353	-1.165276	2.458415
C	2.172665	-0.451867	-1.227418
H	1.905360	-0.253781	-2.264550
C	2.028407	0.105301	1.110252
H	1.655920	0.740906	1.911136
C	1.664194	0.380589	-0.219738
C	0.788741	1.595295	-0.569101
H	0.594142	1.518975	-1.663747
O	1.381008	2.797188	-0.223495
C	-0.594938	1.504005	0.105539
H	-0.507433	1.476083	1.196158
H	-1.201023	2.366880	-0.184828